RNA hydrolysis at mineral-water interfaces

Ke Zhang,[1] Kun-Pu Ho,[1] Anamika Chatterjee,[1] Grace Park,[1] Zhiyao Li,[1] Jeffrey G. Catalano,[2] Kimberly M. Parker[1*]

[1]Department of Energy, Environmental & Chemical Engineering, Washington University in St. Louis, St. Louis, Missouri 63130, United States

[2]Department of Earth & Planetary Sciences, Washington University in St. Louis, St. Louis, Missouri 63130, United States

*Corresponding author: Kimberly M. Parker

Email: kmparker@wustl.edu

Keywords: abiotic RNA hydrolysis, mineral-catalyzed RNA hydrolysis, phosphodiester bond cleavage

This PDF file includes:

Main Text

Figures 1 to 4

Abstract

The adsorption of DNA at mineral-water interfaces is well-established to increase its persistence in soils and sediments; however, adsorbed RNA in similar environments degrades rapidly, in some cases outpacing solution-phase degradation occurring over hours to days. Herein, we elucidate a novel abiotic mechanism by which RNA, but not DNA, degrades upon adsorption to surfaces of iron (oxyhydr)oxides such as goethite (α-FeOOH) that are abundant in soils and sediments. Upon adsorption to goethite, both single-stranded and double-stranded RNA hydrolyzed on the timescale of hours under environmentally relevant physicochemical conditions. The reaction products were consistent with iron present in goethite acting as a Lewis acid to accelerate non-selective hydrolysis of phosphodiester bonds comprising the RNA backbone. In contrast to well-established acid- or base-catalyzed RNA hydrolysis in solution, mineral-catalyzed hydrolysis was fastest at circumneutral pH, which allowed for both sufficient RNA adsorption and hydroxide concentration. We further confirmed that contact of the RNA with the mineral surface is necessary for hydrolysis to occur by demonstrating RNA degradation was inhibited by compact RNA conformation at elevated ionic strength and competitive adsorption with orthophosphate and organic matter. In addition to goethite, we observed RNA hydrolysis was also catalyzed by hematite (α-Fe_2O_3), but not by aluminum-containing minerals (e.g., montmorillonite). Given the extensive adsorption of nucleic acids to environmental surfaces, we anticipate previously overlooked mineral-catalyzed hydrolysis of RNA may be prevalent particularly in iron-rich soils and sediments, which must be considered across biogeochemical applications of nucleic acid analysis in environmental systems.

Introduction

The environmental degradation of DNA has been widely studied due to its broad range of applications, including the measurement of environmental DNA in ecological surveys (1-3), the prevalence of antibiotic resistance genes in the environment (4), the detection of ancient genetic elements in archeology (i.e., ancient DNA) (5), and the elemental cycling of organic phosphorous (6). The extensive adsorption of DNA to minerals in soils and sediments (7) has been consistently demonstrated to dramatically increase the persistence of DNA across numerous studies over decades of research (7-14). For example, to achieve the same extent of enzymatic degradation as dissolved DNA, adsorbed DNA required incubation with orders of magnitude higher nuclease concentrations (10, 12) and, in some cases, was permanently retained over the experiment duration (9). The persistence of adsorbed DNA in environmental systems has largely been attributed to reduced ability of nucleases in the environment to recognize or interact with DNA (13, 15). This protective effect of adsorption has been widely invoked to explain DNA persistence in the environment across disciplines (1-5).

In recent years, RNA persistence in the environment has also gained increasing interest due to its relevance to an array of emerging applications. Environmental RNA has been used to analyze gene expression of microbial communities and improve resolution of biological monitoring. (1, 16). The persistence of viral RNA has also been employed to quantify the abundance of pathogenic viruses including SARS-CoV-2 in water and wastewater systems (17-19). Non-coding RNA has also emerged in environmental contexts due to its potential role in cross-species interactions in soils (20, 21) as well as its development as a pesticidal agent for use in agriculture (22, 23), where its persistence in receiving environments may result in increased risk to non-target species (24). Due to its high abundance in cells, released RNA may also contribute to phosphorous cycling in some environmental systems (1).

Relative to DNA, the presence of the 2′-hydroxyl group on the RNA structure reduces its chemical stability by facilitating hydrolysis of the phosphodiester backbone. However, despite this structural instability, solution-phase abiotic RNA hydrolysis catalyzed by hydroxide or metal ions has

been found to be too slow to contribute to RNA degradation on relevant timescales (i.e., days) in environmental systems (25, 26), suggesting that loss of dissolved RNA predominantly results from microbial nucleases (27). Like DNA, RNA has been observed to strongly adsorb to minerals (e.g., iron (oxyhydr)oxides) (28) and to undergo rapid and extensive adsorption to particles in soils (29, 30). Analogous to DNA, RNA adsorbed to a synthetic clay nanoparticle was established to be protected from nucleases (22). However, in apparent contradiction to the well-established protective effect of adsorption, RNA adsorbed to particles in soil undergoes rapid degradation, in some cases exceeding rates of solution-phase degradation in the same sample (29, 30).

We hypothesized that the apparent instability of adsorbed RNA may be attributable to the hydrolysis of phosphodiester bonds occurring at mineral-water interfaces. Notably, RNA hydrolysis is established to be catalyzed by dissolved metal ions acting as Lewis acids (26, 31), albeit at concentrations far higher than encountered in environmental systems (26). However, metals in certain minerals (i.e., iron (oxyhydr)oxides such as goethite) that are ubiquitous in soils and sediments may facilitate an analogous reaction for RNA adsorbed on mineral surfaces. Consequently, herein we investigated the potential for mineral-catalyzed hydrolysis to contribute to rapid and specific degradation of adsorbed RNA molecules in the environment.

Result and Discussion:

1. Hydrolysis of RNA at the goethite-water interface

To investigate hydrolysis of RNA at the goethite-water interface, unique challenges arising from the strong adsorption of nucleic acids to goethite necessitated careful design of experimental protocols (**Figure 1A**). In solutions with circumneutral pH values, adsorption of nucleic acids to goethite is strongly favored due to electrostatic attraction between negatively charged nucleic acids and net positively charged goethite (point of zero charge = 9.1, **Table S5**), as well as coordination between phosphate groups in nucleic acids and iron atoms on goethite surface (32-34). As polymers, nucleic acid adsorption is further favored due to their interaction with the surface at multiple binding sites (35). These factors contribute to

near-complete adsorption of nucleic acids to unsaturated goethite surfaces within minutes of mixing (30). To ensure nucleic acids were predominantly adsorbed for the duration of the incubation step (**Section S4**), goethite loading was adjusted so that the total amount of nucleic acid in the sample was 70% of the adsorption capacity in each condition (**Section S4**).

The strong adsorption of nucleic acids to goethite surfaces also challenges extraction prior to the analysis of nucleic acids and their hydrolysis products. Specifically, to ensure sufficient recovery for reliable analysis, extraction of nucleic acids must be carried out over multiple hours (30), which is long relative to timescales for the incubation period. To minimize artefactual degradation during extraction, we adapted a previously developed buffer that included orthophosphate to compete with nucleic acids for binding sites (29, 30). However, we decreased its pH value from highly alkaline to neutral matching the value used during incubation to avoid potential pH-dependent effects on hydrolysis occurring during the extract step and increased the ionic strength by adding sodium chloride (NaCl) to reduce potential goethite-catalyzed RNA hydrolysis based on initial trials. We determined extraction periods of 24 h were required to consistently obtain recoveries greater than 70% (**Figures S5, S6**). During extraction, a fraction of nucleic acids remains adsorbed and continues to hydrolyze (**Figures 1A, S9**). Across all experiments, we held the duration of the extraction period constant, resulting in a consistent increase in hydrolysis extent across samples. The amount of additional RNA hydrolyzed during extraction is reflected by a non-zero intercept visible in the kinetics data (e.g., **Figure 1B**).

At increasing incubation time, we observed decreasing concentrations of recovered intact ssRNA in the extract, which is defined as the pool of molecules with lengths that are >75% of the length of the initial ssRNA (25). Consistent with kinetics for base-catalyzed hydrolysis (25), the amount of intact ssRNA decreases following apparent first-order kinetics (**Figure 1B**). The dependency of the rate on ssRNA length was also consistent between the base- (25) and goethite-catalyzed hydrolysis: specifically, increasing the length of the initial molecule by 10-fold resulted in a proportional increase in rate constants for each pathway (i.e., 0.010(±0.001) h^{-1} and 0.14(±0.01) h^{-1} for 106 and 1006 nucleotide (nt) ssRNA,

114 respectively, in **Figure 1B**). In either case, the half-lives for goethite-catalyzed hydrolysis (i.e., 70 and 5 h
115 for 106 and 1006 nt ssRNA, respectively) were far shorter than the timescales required for ssRNA to
116 degrade abiotically in the absence of goethite. For example, RNA remained intact for multiple months or
117 longer without goethite under similar physicochemical conditions (i.e., neutral pH, 24 °C) (25). Notably,
118 these half-lives are comparable to timescales for dissipation of RNA in soils and sediments (25, 27, 36,
119 37).

120 Beyond ssRNA, adsorption at the goethite-water interface also promoted hydrolysis of dsRNA,
121 but not double-stranded DNA (dsDNA) (**Figure 1C**). The apparent first-order rate constant of dsRNA
122 hydrolysis (i.e., 0.052(±0.001) h^{-1}) was ~3-fold slower (**Figure S10**) than ssRNA of a comparable length
123 and sequence (**Section S2**). The duplex structure of dsRNA is known to impede abiotic hydrolysis
124 catalyzed by bases or metal ions (25, 26). Notably, rates for the hydrolysis of dsRNA, if detected at all, by
125 these solution-phase reactions were at least one magnitude slower than for ssRNA, prohibiting these
126 abiotic reactions from contributing significantly to dsRNA degradation in the environment. In contrast,
127 while the hydrolysis of dsRNA at the goethite-water interface was slower than ssRNA, the half-life of the
128 reaction (13 h) remained within the timescales for RNA dissipation in the environment, indicating that
129 mineral-catalyzed hydrolysis may be uniquely capable of degrading dsRNA as well as ssRNA.

130 Unlike dsRNA, dsDNA did not undergo measurable hydrolysis at the goethite-water interface
131 (**Figure 1C**). We hypothesize that this difference may result from the fact that DNA lacks of the 2′-
132 hydroxyl group found in RNA, which facilitates hydrolysis (38). Consequently, although both nucleic
133 acids adsorb strongly to the goethite-water interface (32), mineral-catalyzed hydrolysis is likely to lead to
134 the rapid and selective degradation of RNA molecules over DNA.

135 To validate that hydrolysis of RNA adsorbed to goethite occurred via an abiotic process (i.e., as
136 opposed to degradation by RNase introduced with the goethite), we compared the products of RNA
137 hydrolysis to other known abiotic and biotic hydrolysis pathways. Both intermediate products (i.e.,
138 shorter molecules) and ultimate products (i.e., mononucleotides) differ when generated by abiotic or

biotic hydrolysis of RNA. Specifically, abiotic hydrolysis results in relatively non-selective product distributions, whereas enzymes involved in biotic reactions preferentially generate certain products.

To compare intermediate products, we plotted the intensity of a gel image as a function of migration distance beyond the original ssRNA (29). Shorter ssRNA molecules generated by abiotic alkaline hydrolysis fell along a smooth distribution of lengths with no discernable specific peaks (**Figure 1D**), consistent also with products from abiotic metal ion-catalyzed hydrolysis (26). In contrast, enzymes from representative sources (i.e., human saliva, soil) each generate multiple specific peaks due to preferential scission of specific sequences (**Figure 1E**). The smooth product distribution observed for RNA products extracted from goethite (**Figure 1D**) is therefore suggestive of an abiotic hydrolysis pathway.

Nucleoside monophosphates (NMP) (i.e., adenosine monophosphate (AMP)) generated from RNA hydrolyzed at the goethite-water interface were also consistent with abiotic hydrolysis (**Figure 1F**). Because NMP generation is a slow process requiring numerous phosphodiester bonds to be cleaved, both ssRNA and dsRNA were incubated at the goethite-water interface for longer durations than above experiments (**Figure 1B-1E**). After 190 d of incubation, 4.87(±0.03) μM total AMP was extracted from the goethite, corresponding to ~30% of the AMP added as ssRNA (**Figure 1F**). Less AMP (1.85(±0.00) μM) was recovered from dsRNA, consistent with slower hydrolysis rates. From both ssRNA and dsRNA, AMP isomers were distributed at a ratio of ~0.5-0.6:1 2′-AMP:3′-AMP. This ratio is intermediate between previously reported isomer product ratios for abiotic hydrolysis catalyzed by alkaline pH (~0.8:1.1, indicating a near-random distribution) (25, 39) and metal ions (0.1-0.4:1) (26, 31) (**Figure 1G**). In comparison, enzymatic hydrolysis exclusively generates the 3′-AMP product (40), which is inconsistent with the ratio of isomers recovered from goethite.

2. Solution conditions influence RNA hydrolysis

The effect of solution chemistry – i.e., pH, ionic strength, and presence of competitive adsorbates – on RNA hydrolysis at the goethite-water interface was evaluated for mechanistic insight, as well as to

elucidate factors that may influence the reaction in the environment. Changes to the solution chemistry were made exclusively during the incubation period, while extraction conditions remained constant (**Figure 1A**). For each pH and ionic strength condition, goethite loading was adjusted to keep RNA near-completely in the adsorbed state by maintaining RNA at 70% of the measured solution-specific adsorption capacity (**Section S4**).

Both ssRNA and dsRNA hydrolyzed to the greatest extent when the solution pH was pH 7 rather than either pH 5 or 9 (**Figure 2A**). Decreased hydrolysis at lower pH may indicate involvement of hydroxide in the reaction, while decreased hydrolysis at higher pH resulted from less contact between the RNA and goethite. Although goethite loads were increased at pH 9 to ensure RNA was almost exclusively adsorbed, adsorbed RNA molecules may adopt a conformation at the goethite-water interface that has fewer binding sites, thereby slowing the reaction. In addition, looser binding at high pH during incubation may have resulted in faster release of RNA molecules during extraction despite the use of a neutral pH buffer during the extraction step. Across all pH values, RNA hydrolysis was measurable, suggesting the broad relevance of this reaction at environmentally relevant pH values.

Hydrolysis of ssRNA and dsRNA at the goethite-water interface also occurred across solutions prepared at different ionic strengths (**Figure 2B**). For both RNA types, elevated ionic strength decreased the extent of hydrolysis. Increasing ionic strength leads to charge screening among the negatively charged phosphodiester groups, resulting in RNA adopting a more compact configuration with fewer sites of contact with the goethite surface for each RNA molecule which may slow hydrolysis (32) .

The inclusion of soil-relevant solution constituents (i.e., organic matter, OM; orthophosphate) that compete with RNA for adsorption sites (32) confirmed the importance of contact between RNA and goethite. After goethite was pre-incubated with OM or orthophosphate sufficient to block adsorption sites (**Section S4**), RNA no longer measurably adsorbed to goethite, so we instead investigated measured intact RNA concentration in solution. When incubated with OM-coated goethite, dissolved ssRNA concentrations only marginally declined (~15% over 20 h, **Figure 2C**). The minimal loss of ssRNA may

result from degradation (e.g., by abiotic or enzymatic constituents introduced with the OM) or slow adsorption (e.g., to goethite upon replacement of OM or to the OM itself). The inclusion of orthophosphate had an even more pronounced effect on ssRNA stability in the solution phase (**Figure 2D**). No loss was measured over 12 d, possibly due to fewer contaminants introduced with the phosphate than OM or more complete and irreversible blocking of sorption sites on the goethite surface. Consequently, catalyzed hydrolysis of RNA in the presence of goethite appears to specifically require adsorption of RNA at the mineral-water interface.

3. RNA hydrolysis catalyzed by other minerals

We next evaluated the capacity of minerals beyond goethite to catalyze RNA hydrolysis. Among the six additional minerals tested, silica (SiO_2) neither adsorbed nor hydrolyzed RNA (**Section S5**) and so was not investigated further. The other five minerals – including the iron oxide hematite (α-Fe_2O_3), the aluminum (oxyhydr)oxides gibbsite (γ-$Al(OH)_3$) and aluminum oxide (Al_2O_3), and the clays montmorillonite and kaolinite – all adsorbed RNA (**Section S4**). To improve RNA recovery from these diverse minerals, the pH of the extraction buffer was increased to 11.5 (**Figure 3**), which necessitated the use of dsRNA instead of ssRNA to avoid alkaline hydrolysis (25).

After 0.5 h of incubation, ~50% and ~100% of dsRNA was recovered from hematite and montmorillonite respectively (**Figure 3A,B**). After 30 h, the recovery of total RNA (i.e., including hydrolyzed products contributing to light absorbance at 260 nm) from hematite remained ~50%, but the amount of intact dsRNA decreased to ~20% of the added amount. The lower amount of intact dsRNA relative to total RNA indicated that hematite, an iron-containing mineral like goethite, also catalyzed RNA hydrolysis. In contrast, the recovery of intact dsRNA from montmorillonite remained near 100% even after 120 h. Montmorillonite may be unable to catalyze RNA hydrolysis because RNA adsorption is limited to electrostatic interactions (41, 42), whereas iron (oxyhydr)oxides also coordinate phosphate groups in RNA (32-35).

The remaining minerals strongly adsorbed dsRNA and did not permit extraction even using the alkaline buffer (**Section S5**). Further modification of the adsorption buffer allowed dsRNA extraction from kaolinite and gibbsite, but not aluminum oxide, which was excluded from further study (**Section S5**). The required changes to the adsorption buffer to allow dsRNA extraction (lower pH, high ionic strength) also disfavor RNA hydrolysis on goethite (**Figure 2**), likely corresponding to looser binding between the RNA and the mineral in both cases. Close agreement between the recoveries (ranging from 34-56%) of total and intact RNA after 120 h in each case suggest that RNA did not hydrolyze when adsorbed to either kaolinite or gibbsite under these conditions. Although, like goethite, these minerals may coordinate phosphate groups, phosphate that readily desorbs is instead bound via weaker electrostatic attraction (41, 42) that may not facilitate RNA hydrolysis. While the non-recoverable fraction of adsorbed RNA may undergo coordination and therefore hydrolyze, the relevance of RNA degradation by these minerals is likely limited due to its irreversible adsorption under most conditions relevant to the environment.

4. Proposed mechanism of mineral-catalyzed RNA hydrolysis

From our results, we propose that hydrolysis of mineral-adsorbed RNA is enabled by the coordination between iron atoms in iron (oxyhydr)oxides and phosphate groups in RNA (**Figure 4**). The lack of RNA hydrolysis when adsorption was prevented by competitors (i.e., organic matter, orthophosphate) (**Figure 2C,D**) supports surface-bound RNA as the primary fraction undergoing hydrolysis in the presence of iron (oxyhydr)oxides. Hydrolysis occurred when RNA was adsorbed to iron (oxyhydr)oxides like goethite known to bind nucleic acids by coordination between surface iron atoms and phosphate groups (32-35), but not when RNA was adsorbed to montmorillonite (**Figure 3B**), which binds nucleic acids exclusively by electrostatic interactions (42). Coordination of phosphate groups to surface metal atoms may facilitate RNA hydrolysis by drawing electron density away from the phosphorous atom, thereby increasing its electrophilicity. Dissolved metal ions that act as Lewis acids (e.g., Pb^{2+}, Zn^{2+}) are known to catalyze dissolved RNA via an analogous solution-phase mechanism (31, 43), which has also been invoked to explain the hydrolysis of organic compounds containing

phosphoester bonds on mineral surfaces (44-48). Like iron, aluminum atoms also form coordination bonds with phosphate groups (42); however, phosphate groups bound via coordination do not desorb readily from gibbsite and kaolinite (42), which may explain why RNA extracted from these minerals did not exhibit hydrolysis (**Figure 3C,D**).

While metal coordination is sufficient to catalyze hydrolysis of certain organic compounds containing phosphoester bonds (44-48), the specificity of goethite-catalyzed hydrolysis for RNA relative to DNA (**Figure 1C**) indicates the additional involvement of the 2′-hydroxyl group that is present in RNA but absent in DNA. Deprotonation of the 2′-hydroxyl group forms an oxyanion, which is a strong nucleophile that subsequently attacks the phosphorous atom (38), leading to cleavage of the phosphodiester bond (**Figure 4**). The intramolecular nucleophilic attack of the 2′-oxyanion is well-established to contribute to rapid hydrolysis of dissolved RNA in alkaline conditions (38), although it is impeded in duplex molecules (25), which may contribute to slower hydrolysis of dsRNA relative to ssRNA on goethite surfaces (**Figure 1B,C**). Support for the involvement of 2′-oxyanion in mineral-catalyzed hydrolysis is also provided by decreased hydrolysis of RNA at acidic pH values relative to neutral conditions (**Figure 2A**). The ultimate monomeric products of mineral-catalyzed RNA hydrolysis are generated at an isomeric ratio (i.e., [2′-NMP]/[3′-NMP]) that falls between ratios generated by RNA hydrolysis catalyzed by alkaline conditions (which favor the 2′-oxyanion) and dissolved metal ions (which increase the electrophilicity of the phosphorous atom) (**Figure 1G**), consistent with both factors contributing to RNA hydrolysis on the mineral surface.

Implications:

The hydrolysis of RNA adsorbed onto iron (oxyhydr)oxides is the first abiotic hydrolysis pathway demonstrated to contribute to RNA degradation on relevant timescales (e.g., days) at environmentally relevant conditions. Furthermore, because the rapid adsorption of RNA to these minerals likely protects RNA from enzymatic degradation (22), mineral-catalyzed hydrolysis is likely the most important degradation pathway for adsorbed RNA, which accounts for a large fraction of RNA in soils

and sediments (29). This fate process may be particularly important in iron oxide-rich soils like Utisols, which account for approximately one-tenth of globally ice-free land (49).

The potential for mineral-catalyzed hydrolysis to contribute to selective degradation of RNA relative to DNA must be considered when applying nucleic acid quantification in soils and sediments to ecological analysis. For example, extracted RNA may be biased lower relative to DNA when comparing transcriptomic to genomic data (1, 16) and RNA to DNA viral abundances (18, 19). The hydrolysis of adsorbed RNA may also limit the environmental persistence of noncoding RNA serving for natural inter-species interactions (20, 21) and as engineered biopesticides in agriculture (22, 23). In all of these applications, adsorbed RNA must be returned to the solution phase to be either quantified or bioavailable. Consequently, the degradation of extractable RNA adsorbed to minerals like iron (oxyhydr)oxides that catalyze hydrolysis may be particularly relevant in comparison to non-extractable RNA that is strongly bound to aluminum (oxyhydr)oxides.

The hydrolysis of adsorbed RNA may also be important for phosphorous cycling, particularly due to greater releases of RNA relative to DNA upon cell death (1). Both DNA and RNA are phosphorous-rich biomolecules that serve as major pools of organic phosphorus in some environmental systems (i.e., deep-sea top sediments (6)). Mineral-catalyzed hydrolysis of adsorbed RNA may return organic phosphorous to solution by converting RNA polymers to hydrolysis products that are more weakly bound to the mineral surface (35). Hydrolysis products may also be released upon iron reduction, thereby contributing to phosphorous cycling in fluctuating redox environments (e.g., forest soils, agricultural soils, estuarine sediments) (50-52).

Materials and Methods

1. Chemicals & Supplies

All chemicals and supplies used in this study are detailed in **Section S1**. Nucleic acids (i.e., 1023 base pair (bp) DNA, 1000 bp dsRNA, 1006 nt ssRNA, 106 nt ssRNA; sequences provided in **Section S2**) were synthesized using prior protocols employing polymerase chain reaction (PCR) for DNA synthesis

and in vitro T7 polymerase for RNA synthesis (25, 30). We modified the final step of the DNA synthesis protocol so that the DNA product was eluted in molecular grade water to avoid experimental interference arising from constituents in the prior elution buffer (10 mM Tris-HCl, pH 8.5).

Goethite, aluminum oxide, and silica were used directly as obtained from commercial sources (**Section S3**). Montmorillonite and kaolinite from the Clay Minerals Society Source Clays Repository were pretreated to remove carbonate and retain fractions smaller than 2 μm (**Section S3**). Hematite and gibbsite were synthesized (**Section S3**). Minerals were analyzed to determine surface area, point of zero charge and (if synthesized) crystal structure. (**Section S3**).

We minimized the unintentional presence of RNase in our experiments using a prior protocol (25). Specifically, we used RNase-free disposable supplies (e.g., tubes and pipettor tips), baked glassware (450 °C, 4 h), or reusable plasticware treated with 0.1% diethylpyrocarbonate (DEPC) for 8 h, followed by autoclaving to decompose DEPC. Buffers were prepared with ultrapure water, autoclaved, and aliquoted before storage at 4 °C (for <1 week) or at -20 °C (for long term storage). All synthesis and experimental steps involving RNA prior to analysis were carried out in a laminar hood. Among materials used in this study, only minerals and organic matter (Suwannee River Natural Organic Matter) were not DEPC-treated nor autoclaved to avoid potential alterations to their chemical structures. However, all preparatory and pre-treatment steps for these materials exclusively used treated solutions and supplies. Organic matter solutions were additionally filtered through 0.22 μm membrane filters to remove particles and microbes. Experimental results described in detail above are consistent with minimal contributions of RNase to RNA degradation.

2. Experimental Design & Analysis

During the incubation phase (**Figure 1A**), 23.3 ng/μL nucleic acid was adsorbed to minerals in 100 μL (silica and aluminum oxide) or 60 μL (all other minerals) solutions that contained 10 mM NaCl and was buffered at pH 7 by 3 mM 3-(4-morpholino)propane sulfonic acid (MOPS). Mineral loadings

were selected so that nucleic acids were present at 70% of their adsorption capacity for specific mineral and solution conditions (**Section S4**).

Samples were agitated using a Thermomixer at 800 rpm and 25 °C for the duration of the incubation period, then centrifuged (21,100 g, 5 min) before the solution was exchanged with the extraction buffer to liberate adsorbed nucleic acids (**Figure 1A**). An extraction buffer containing 3 mM MOPS (pH 7), 100 mM NaCl, and 12 mM phosphate recovered ~75% of nucleic acids adsorbed to goethite (determined by solution absorbance measurements), independent of incubation time, nucleic acid type, or buffer composition (**Section S5**). Other minerals required the use of different extraction conditions (**Figure 4**, **Section S5**).

To quantify the aggregate concentrations of nucleic acids and hydrolysis products (i.e., for recovery estimates) in supernatants, we measured ultraviolet (UV) light absorbance – primarily contributed by nucleobases uninvolved in hydrolysis – using a NanoDrop 2000c spectrophotometer (Thermo Fisher Scientific). Total concentrations of DNA, dsRNA, and ssRNA were estimated from UV absorbance at 260 nm using extinction coefficients of 0.0216, 0.0214 and 0.0266 $(ng/\mu L)^{-1} \cdot cm^{-1}$, respectively (53). We measured loss of intact nucleic acids due to hydrolysis using agarose gel electrophoresis with image analysis using a prior validated protocol (25). AMP concentrations were determined using high-performance liquid chromatography (HPLC) with UV detection (25).

Acknowledgments

This work is supported by the USDA Biotechnology Risk Assessment Grant Program Award 2017-33522-26998 (K.M.P.), NSF CAREER Award 2046602 (K.M.P.), American Chemical Society - Petroleum Research Fund 60057-DNI4 (K.M.P.), and the NASA Astrobiology Program Award No. 80NSSC19M0069 (J.G.C.). We thank Yao Ma and Daniel Giammar for determining the crystal structure of synthesized minerals. We thank Fuzhong Zhang for access to the gel image system.

Author Contributions

K.Z. and K.M.P designed the research; K.Z., K.P.H., G.P., and Z.L. conducted the experiments; A.C. conducted the HPLC analysis; J.G.C. supported the selection and characterization of minerals; K.Z. analyzed the data; all authors wrote and approved the manuscript.

Competing Interest Statement

The authors declare no competing financial interest.

References

1. A. Torti, M. A. Lever, B. B. Jørgensen, Origin, dynamics, and implications of extracellular DNA pools in marine sediments. *Mar. Genomics* **24**, 185-196 (2015).
2. P. Carini, P. J. Marsden, J. W. Leff, E. E. Morgan, M. S. Strickland, N. Fierer, Relic DNA is abundant in soil and obscures estimates of soil microbial diversity. *Nat. Microbiol.* **2**, 16242 (2016).
3. Q. Mauvisseau, L. R. Harper, M. Sander, R. H. Hanner, H. Kleyer, K. Deiner, The Multiple States of Environmental DNA and What Is Known about Their Persistence in Aquatic Environments. *Environ. Sci. Technol.* **56**, 5322-5333 (2022).
4. D. Mao, Y. Luo, J. Mathieu, Q. Wang, L. Feng, Q. Mu, C. Feng, P. J. J. Alvarez, Persistence of Extracellular DNA in River Sediment Facilitates Antibiotic Resistance Gene Propagation. *Environ. Sci. Technol.* **48**, 71-78 (2014).
5. A. Grunenwald, C. Keyser, A. M. Sautereau, E. Crubézy, B. Ludes, C. Drouet, Adsorption of DNA on biomimetic apatites: Toward the understanding of the role of bone and tooth mineral on the preservation of ancient DNA. *Appl. Surf. Sci.* **292**, 867-875 (2014).
6. A. Dell'Anno, R. Danovaro, Extracellular DNA Plays a Key Role in Deep-Sea Ecosystem Functioning. *Science* **309**, 2179-2179 (2005).
7. S. A. E. Blum, M. G. Lorenz, W. Wackernagel, Mechanism of Retarded DNA Degradation and Prokaryotic Origin of DNases in Nonsterile Soils. *Syst. Appl. Microbiol.* **20**, 513-521 (1997).
8. B. W. Aardema, M. G. Lorenz, W. E. Krumbein, Protection of Sediment-Adsorbed Transforming DNA Against Enzymatic Inactivation. *Appl. Environ. Microbiol.* **46**, 417-420 (1983).
9. M. G. Lorenz, W. Wackernagel, Adsorption of DNA to sand and variable degradation rates of adsorbed DNA. *Appl. Environ. Microbiol.* **53**, 2948-2952 (1987).
10. G. Romanowski, M. G. Lorenz, W. Wackernagel, Adsorption of plasmid DNA to mineral surfaces and protection against DNase I. *Appl. Environ. Microbiol.* **57**, 1057-1061 (1991).

11. E. Paget, L. J. Monrozier, P. Simonet, Adsorption of DNA on clay minerals: protection against DNaseI and influence on gene transfer. *FEMS Microbiol. Lett.* **97**, 31-39 (1992).
12. M. Khanna, G. Stotzky, Transformation of Bacillus subtilis by DNA bound on montmorillonite and effect of DNase on the transforming ability of bound DNA. *Appl. Environ. Microbiol.* **58**, 1930-1939 (1992).
13. M. G. Lorenz, W. Wackernagel, Bacterial gene transfer by natural genetic transformation in the environment. *Microbiol. Rev.* **58**, 563-602 (1994).
14. P. Cai, Q.-Y. Huang, X.-W. Zhang, Interactions of DNA with Clay Minerals and Soil Colloidal Particles and Protection against Degradation by DNase. *Environ. Sci. Technol.* **40**, 2971-2976 (2006).
15. G. Stotzky, Persistence and Biological Activity in Soil of Insecticidal Proteins from Bacillus thuringiensis and of Bacterial DNA Bound on Clays and Humic Acids. *J. Environ. Qual.* **29**, 691-705 (2000).
16. M. C. Yates, A. M. Derry, M. E. Cristescu, Environmental RNA: A Revolution in Ecological Resolution? *Trends Ecol. Evol.* **36**, 601-609 (2021).
17. D. A. Larsen, K. R. Wigginton, Tracking COVID-19 with wastewater. *Nat. Biotechnol.* **38**, 1151-1153 (2020).
18. A. I. Silverman, A. B. Boehm, Systematic Review and Meta-Analysis of the Persistence and Disinfection of Human Coronaviruses and Their Viral Surrogates in Water and Wastewater. *Environ. Sci. Technol. Lett* **7**, 544-553 (2020).
19. A. I. Silverman, A. B. Boehm, Systematic Review and Meta-Analysis of the Persistence of Enveloped Viruses in Environmental Waters and Wastewater in the Absence of Disinfectants. *Environ. Sci. Technol.* **55**, 14480-14493 (2021).
20. I. de Bruijn, K. J. F. Verhoeven, Cross-species interference of gene expression. *Nat. Commun.* **9**, 5019 (2018).

21. C.-Y. Huang, H. Wang, P. Hu, R. Hamby, H. Jin, Small RNAs – Big Players in Plant-Microbe Interactions. *Cell Host Microbe* **26**, 173-182 (2019).

22. N. Mitter, E. A. Worrall, K. E. Robinson, P. Li, R. G. Jain, C. Taochy, S. J. Fletcher, B. J. Carroll, G. Q. Lu, Z. P. Xu, Clay nanosheets for topical delivery of RNAi for sustained protection against plant viruses. *Nat. Plants* **3**, 16207 (2017).

23. J. A. Baum, T. Bogaert, W. Clinton, G. R. Heck, P. Feldmann, O. Ilagan, S. Johnson, G. Plaetinck, T. Munyikwa, M. Pleau, T. Vaughn, J. Roberts, Control of coleopteran insect pests through RNA interference. *Nat. Biotechnol.* **25**, 1322-1326 (2007).

24. K. M. Parker, M. Sander, Environmental Fate of Insecticidal Plant-Incorporated Protectants from Genetically Modified Crops: Knowledge Gaps and Research Opportunities. *Environ. Sci. Technol.* **51**, 12049-12057 (2017).

25. K. Zhang, J. Hodge, A. Chatterjee, T. S. Moon, K. M. Parker, Duplex Structure of Double-Stranded RNA Provides Stability against Hydrolysis Relative to Single-Stranded RNA. *Environ. Sci. Technol.* **55**, 8045-8053 (2021).

26. A. Chatterjee, K. Zhang, Y. Rao, N. Sharma, D. E. Giammar, K. M. Parker, Metal-Catalyzed Hydrolysis of RNA in Aqueous Environments. *Environ. Sci. Technol.* **56**, 3564–3574 (2022).

27. J. R. Fischer, F. Zapata, S. Dubelman, G. M. Mueller, J. P. Uffman, C. Jiang, P. D. Jensen, S. L. Levine, Aquatic fate of a double-stranded RNA in a sediment-–-water system following an over-water application. *Environ. Toxicol. Chem.* **36**, 727-734 (2017).

28. U. Schwertmann, "Relations Between Iron Oxides, Soil Color, and Soil Formation" in Soil Color. (1993), pp. 51-69.

29. K. M. Parker, V. Barragán Borrero, D. M. van Leeuwen, M. A. Lever, B. Mateescu, M. Sander, Environmental fate of RNA interference pesticides: Adsorption and degradation of double-stranded RNA molecules in agricultural soils. *Environ. Sci. Technol.* **53**, 3027-3036 (2019).

30. K. Zhang, J. Wei, K. E. Huff Hartz, M. J. Lydy, T. S. Moon, M. Sander, K. M. Parker, Analysis of RNA Interference (RNAi) Biopesticides: Double-Stranded RNA (dsRNA) Extraction from Agricultural Soils and Quantification by RT-qPCR. *Environ. Sci. Technol.* **54**, 4893-4902 (2020).
31. V. M. Shelton, J. R. Morrow, Catalytic transesterification and hydrolysis of RNA by zinc(II) complexes. *Inorg. Chem.* **30**, 4295-4299 (1991).
32. K. Sodnikar, K. M. Parker, S. R. Stump, L. K. ThomasArrigo, M. Sander, Adsorption of double-stranded ribonucleic acids (dsRNA) to iron (oxyhydr-)oxide surfaces: comparative analysis of model dsRNA molecules and deoxyribonucleic acids (DNA). *Environ. Sci.: Process. Impacts* **23**, 605-620 (2021).
33. M. P. Schmidt, C. E. Martínez, Supramolecular Association Impacts Biomolecule Adsorption onto Goethite. *Environ. Sci. Technol.* **52**, 4079-4089 (2018).
34. M. P. Schmidt, C. E. Martínez, Ironing Out Genes in the Environment: An Experimental Study of the DNA–Goethite Interface. *Langmuir* **33**, 8525-8532 (2017).
35. N. G. Holm, G. Ertem, J. P. Ferris, The binding and reactions of nucleotides and polynucleotides on iron oxide hydroxide polymorphs. *Orig. Life Evol. Biosph.* **23**, 195-215 (1993).
36. S. Dubelman, J. Fischer, F. Zapata, K. Huizinga, C. Jiang, J. Uffman, S. Levine, D. Carson, Environmental fate of double-stranded RNA in agricultural soils. *PLoS One* **9**, e93155 (2014).
37. M. B. Kunadiya, T. I. Burgess, W. A. Dunstan, D. White, G. E. StJ. Hardy, Persistence and degradation of Phytophthora cinnamomi DNA and RNA in different soil types. *Environ. DNA* **3**, 92-104 (2021).
38. Y. Li, R. R. Breaker, Kinetics of RNA Degradation by Specific Base Catalysis of Transesterification Involving the 2'-Hydroxyl Group. *J. Am. Chem. Soc.* **121**, 5364-5372 (1999).
39. M. Komiyama, Y. Takeshige, Regioselective phosphorus-oxygen(3') cleavage of 2',3'-cyclic monophosphates of ribonucleosides catalyzed by β- and γ-cyclodextrins. *J. Org. Chem.* **54**, 4936-4939 (1989).

40. H. Dugas, C. Penney, "Bioorganic Chemistry of the Phosphates" in Bioorganic Chemistry: A Chemical Approach to Enzyme Action. (Springer US, New York, NY, 1981), pp. 93-178.

41. J. P. Ferris, G. Ertem, V. K. Agarwal, The adsorption of nucleotides and polynucleotides on montmorillonite clay. *Orig. Life Evol. Biosph.* **19**, 153-164 (1989).

42. T. J. Van Emmerik, D. E. Sandström, O. N. Antzutkin, M. J. Angove, B. B. Johnson, ^{31}P Solid-State Nuclear Magnetic Resonance Study of the Sorption of Phosphate onto Gibbsite and Kaolinite. *Langmuir* **23**, 3205-3213 (2007).

43. R. Breslow, D. L. Huang, Effects of metal ions, including Mg^{2+} and lanthanides, on the cleavage of ribonucleotides and RNA model compounds. *Proc. Natl. Acad. Sci. U. S. A.* **88**, 4080-4083 (1991).

44. Y. Fang, E. Kim, T. J. Strathmann, Mineral- and Base-Catalyzed Hydrolysis of Organophosphate Flame Retardants: Potential Major Fate-Controlling Sink in Soil and Aquatic Environments. *Environ. Sci. Technol.* **52**, 1997-2006 (2018).

45. A. Torrents, A. T. Stone, Oxide Surface-Catalyzed Hydrolysis of Carboxylate Esters and Phosphorothioate Esters. *Soil Sci. Soc. Am. J.* **58**, 738-745 (1994).

46. P. Mäkie, P. Persson, L. Österlund, Adsorption of trimethyl phosphate and triethyl phosphate on dry and water pre-covered hematite, maghemite, and goethite nanoparticles. *J. Colloid Interface Sci.* **392**, 349-358 (2013).

47. B. Wan, P. Yang, H. Jung, M. Zhu, J. M. Diaz, Y. Tang, Iron oxides catalyze the hydrolysis of polyphosphate and precipitation of calcium phosphate minerals. *Geochim. Cosmochim. Acta* **305**, 49-65 (2021).

48. X.-L. Huang, What are inorganic nanozymes? Artificial or inorganic enzymes. *New J. Chem.* **46**, 15273-15291 (2022).

49. R. R. Weil, N. C. Brady, *The Nature and Properties of Soils, 15th Edition* (Pearson, London, U.K., 2017).

50. T. Peretyazhko, G. Sposito, Iron(III) reduction and phosphorous solubilization in humid tropical forest soils. *Geochim. Cosmochim. Acta* **69**, 3643-3652 (2005).

51. D. L. McRose, D. K. Newman, Redox-active antibiotics enhance phosphorus bioavailability. *Science* **371**, 1033-1037 (2021).

52. H. M. Queiroz, T. O. Ferreira, D. Barcellos, G. N. Nóbrega, J. Antelo, X. L. Otero, A. F. Bernardino, From sinks to sources: The role of Fe oxyhydroxide transformations on phosphorus dynamics in estuarine soils. *J. Environ. Manage.* **278**, 111575 (2021).

53. A. O. Nwokeoji, P. M. Kilby, D. E. Portwood, M. J. Dickman, Accurate Quantification of Nucleic Acids Using Hypochromicity Measurements in Conjunction with UV Spectrophotometry. *Anal. Chem.* **89**, 13567-13574 (2017).

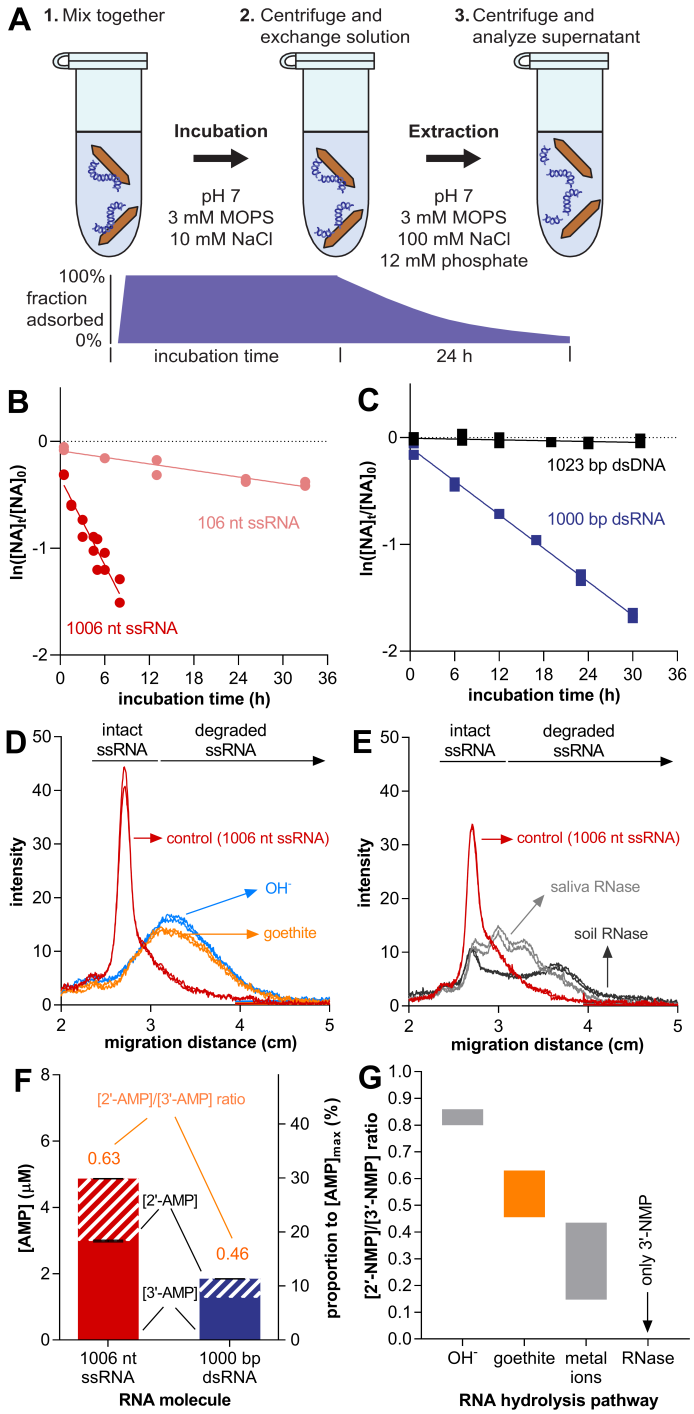

Figure 1. Hydrolysis of RNA adsorbed to goethite. (A) Schematic of the experimental approach depicting fraction of nucleic acids in the adsorbed state at each stage. (**B, C**) Loss of intact ssRNA, dsRNA, and dsDNA adsorbed to goethite. (**D, E**) Intensity plots of control ssRNA (1006 nt) and ssRNA

hydrolyzed by goethite, OH^- (i.e. alkaline pH), saliva RNase, and soil RNase to comparable degradation extents (**Figure S11**)). (**F**) Adenosine monophosphate (AMP) analysis of goethite-catalyzed RNA hydrolysis after 190 d of incubation. $[AMP]_{max}$ denotes the AMP concentration if RNA molecules were fully hydrolyzed to nucleoside monophosphate, which was simplified for presentation as a single value (16.3 μM) that is the average of marginally different values for ssRNA (16.7 μM) and dsRNA (15.9 μM). The concentrations of 3′-AMP from dsRNA in duplicate samples were identical at the instrumental precision level. Samples are prepared in duplicate in (**B**-**F**). Error bars represent standard derivation. (**G**) 3′-nucleoside monophosphates (NMP)/2′-NMP ratios of 3′-NMP/2′-NMP generated from hydrolysis of RNA catalyzed by OH^- (i.e., alkaline pH) (25, 39), goethite (this study), metal ions (31), and RNase (40) as detailed in **Table S5**.

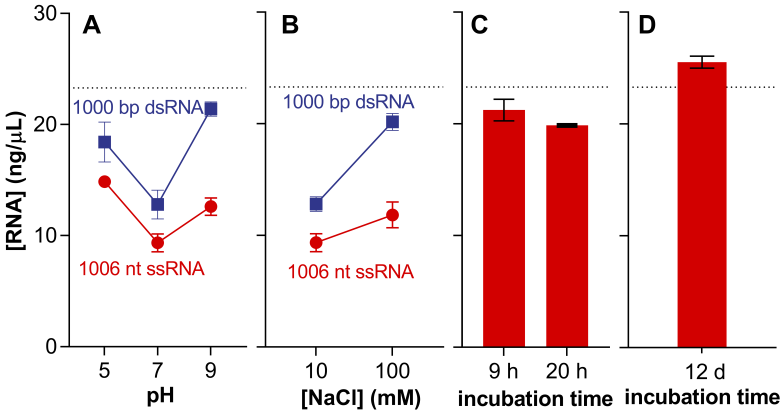

492

493 **Figure 2. Intact RNA recovered from goethite incubated with varying solution chemistry.** (**A**) The
494 pH of the adsorption solution was varied from a value of 7 (3-(4-morpholino)propane sulfonic acid,
495 MOPS) to 5 (acetate) or 9 (tetraborate) with each buffer at 3 mM including 10 mM NaCl. (**B**) Ionic
496 strength was increased using NaCl in solution held at pH 7 with 3 mM MOPS. In (**A**) and (**B**), incubation
497 periods were 2 h (ssRNA) or 10 h (dsRNA), while extraction conditions were maintained constant as
498 depicted in **Figure 1A**. (**C, D**) Goethite was pre-incubated with 0.207 mg-C/mL organic matter (**Figure**
499 **S12**) or 12 mM orthophosphate, followed by RNA (1006 nt) addition (**Section S4**); RNA in the
500 supernatant was analyzed. Error bars represent the standard deviation of measurements from duplicate
501 samples. The dashed line refers to nominal initial RNA concentration.

502

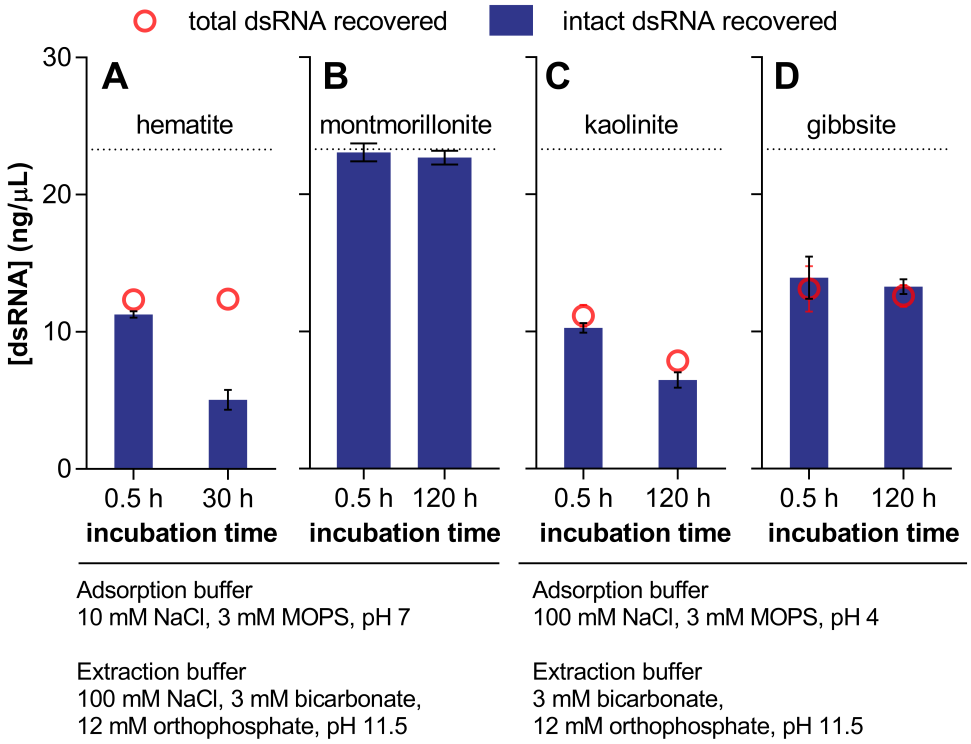

Figure 3. Intact RNA relative to total RNA (i.e., including hydrolyzed products) recovered from hematite (A), montmorillonite (B), kaolinite (C), and gibbsite (D) after adsorption and extraction using specified buffers. Intact RNA recovered was determined by agarose gel electrophoresis. Total RNA recovered was determined by UV absorbance at 260 nm, except for montmorillonite due to dissolved constituents that interfered with solution absorbance. Error bars represent the standard deviation of measurements from duplicate samples. The dashed line refers to the nominal initial RNA concentration.

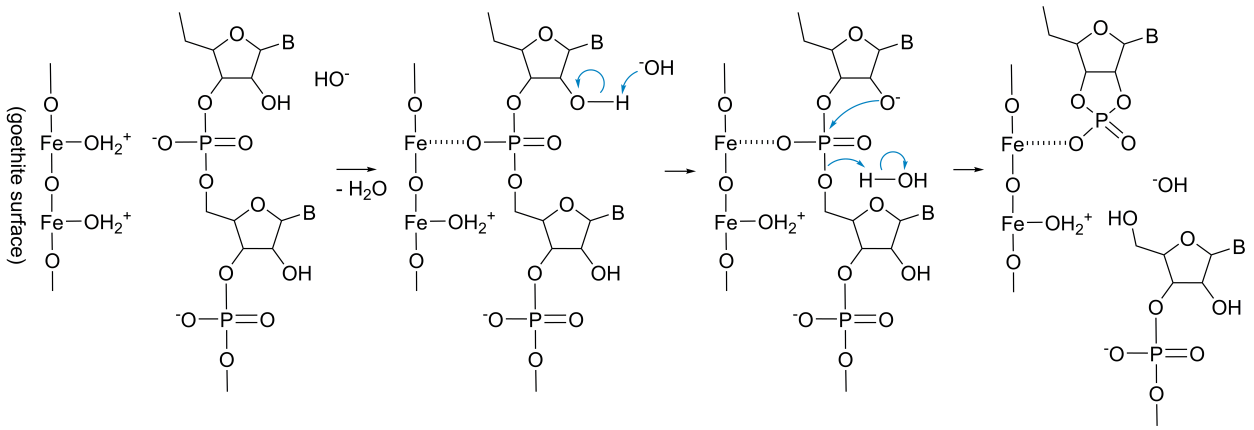

Figure 4. Proposed mechanism of catalyzed RNA hydrolysis on the surface of iron (oxyhydr)oxides (e.g., goethite). Upon RNA adsorption, both the coordination of iron with the phosphate group and the deprotonation of 2′-hydroxyl promote the nucleophilic attack on phosphorus atom leading to the cleavage of the phosphodiester bond.